Kerstin Wilhelm

FOXO1 couples metabolic activity and growth state in the vascular endothelium

Max Planck Institute for Heart and Lung Research, Angiogenesis & Metabolism Laboratory, Bad Nauheim, Germany

Endothelial cells (ECs) line the luminal side of blood vessels. When tissues are in need of oxygen and nutrients they secrete proangiogenic factors, which trigger ECs to become invasive and protrude filopodia. The so-called tip cells lead the sprouts and extend their filopodia towards the source of the angiogenic signal. Tip cells are followed by stalk cells, which proliferate to elongate the sprout. Eventually, tip cells connect with tip cells from adjacent sprouts to establish new vessel circuits. This process of vessel growth from pre-existing vessels is named angiogenesis. Angiogenesis continues until nutrient and oxygen supply meets tissue demand, proangiogenic molecules are silenced, and ECs become quiescent again. Compared to quiescence active sprouting is highly energy demanding[1]. While the tip cells need an extensive amount of ATP, because they have to remodel their cytoskeleton in order to protrude filopodia, stalk cells need to double their biomass in order to be able to divide and proliferate. This suggests that ECs have to adapt their metabolism when switching from quiescence to vascular growth. However, how ECs couple their metabolic activity to growth state is poorly understood at the molecular level.

We analyzed the role of FOXO in the endothelium. FOXO is an effector of the phosphatidylinositol-3-OH kinase (PI(3)K)/AKT pathway that links growth and metabolism. PI(3)K signalling inhibits FOXOs through AKT-mediated phosphorylation leading to their nuclear exclusion. We investigated the role of FOXO1 in ECs, an enriched FOXO family member in the endothelium. To this end, we bred floxed *Foxo1* mice (*Foxo1*$^{fl/fl}$)[2] with a *Tie2-cre* deleter, which recombines in endothelial and haematopoietic cells. *Tie2-cre*-mediated deletion of *Foxo1* (*Foxo1*$^{EC\text{-}KO}$) caused defective vascular development and embryonic lethality around embryonic day (E)10.5[3], suggesting that endothelial FOXO1 is essential for embryo development. Immunofluorescence analysis of developing blood vessels in the postnatal retina showed high levels of FOXO1 expression in the endothelium (Fig. 1a). Further examination of the subcellular distribution revealed a diffuse nucleocytoplasmic localization of FOXO1 at the angiogenic front, where most of the EC proliferation occurs, but a stronger nuclear pattern in the plexus, where vessels remodel, and endothelial proliferation abates (Fig. 1a). This spatial difference in subcellular localization suggests that FOXO1 is important for governing endothelial growth. To test this, we assessed the impact of *Foxo1* deletion on retinal angiogenesis using the tamoxifen-inducible, endothelial-selective *Pdgfb-creERT2* line (*Foxo1*$^{iEC\text{-}KO}$). Endothelial loss of *Foxo1* caused a dense and hyperplastic vasculature and resulted in the inability of ECs to extend proper sprouts (Fig. 1b–f). Instead, ECs grew in clusters leading to vessel enlargement and blunting of the angiogenic front (Fig. 1d, f). Strikingly, numerous filopodial bursts were emanating from the stunted front (Fig. 1c, d), suggesting that FOXO1 deficiency results in uncoordinated vascular growth. Assessment of 5-bromodeoxyuridine (BrdU) incorporation demonstrated a substantial increase in endothelial proliferation in the *Foxo1*$^{iEC\text{-}KO}$ mutants (Fig. 1g, j), indicating that deregulated proliferation drives this aberrant vessel phenotype. Because of the fact that in the majority of mouse mutants the retinal vascular phenotypes resolve during later stages of retinal vascular development, we analyzed the *Foxo1*$^{iEC\text{-}KO}$ mutants at postnatal day 21 (P21) when overall vessel morphogenesis is completed. Importantly, the vascular defects did not normalize at later stages of development, but showed a persistent increase in endothelial number, density and vessel diameter (Fig. 1h, i). We conclude that FOXO1 is a suppressor of endothelial growth and proliferation, whose inactivation leads to uncontrolled overgrowth.

Next, we determined the consequences of FOXO1 activation in ECs. We used a Cre-inducible gain-of-function allele (*Foxo1*^{CA}) in which the AKT phosphorylation sites are mutated, thus rendering FOXO1 constitutively nuclear (Fig. 2b)[4]. *Tie2-cre*-mediated expression of this IRES-GFP-coexpressing mutant (*Foxo1*$^{EC\text{-}CA}$) was incompatible with embryo survival beyond E10.5 (Fig. 2a), highlighting the sensitivity of ECs towards changes in FOXO1 status. We then used the Pdgfb-creERT2 strain to express *Foxo1*^{CA} in the retinal endothelium (*Foxo1*$^{iEC\text{-}CA}$). Immunofluorescence studies revealed an enriched FOXO1 signal in endothelial nuclei and confirmed the EC-specific expression of GFP (Fig. 2b). Forced activation of FOXO1 led to a sparse and hyperpruned vascular network that contained fewer ECs (Fig. 2c, d, f–h). These retinal vessels established a lumen but were thinner (Fig. 2g, h). Staining for phospho-histone H3 (pHH3) revealed a reduction in EC proliferation in *Foxo1*$^{iEC\text{-}CA}$ mice while endothelial apoptosis was not altered (Fig. 2e, f, i). Given the fact that different vascular beds might cope variably with forced FOXO1 expression, we investigated the consequence of FOXO1 activation in the embryonic hindbrain. Similar phenotypes were observed in the hindbrain vasculature (Fig. 2j, k), indicating that FOXO1 is a critical driver of endothelial quiescence.

We next assessed whether FOXO1 regulates endothelial metab-

olism. Since ECs rely on glycolysis for vessel branching[1], we first studied the effects of FOXO1 on this metabolic pathway. Transduction of human umbilical vein endothelial cells (HUVECs) with a FOXO1^{CA}-encoding adenovirus (AdFOXO1^{CA}) led to a robust reduction in glycolysis as evidenced by a reduction in extracellular acidification rate (ECAR), glucose uptake, glycolytic flux and lactate production (Fig. 3a–d). This metabolic phenotype correlates with the reduced proliferation in FOXO1^{CA}-expressing ECs and raises a question as to whether FOXO1 promotes mitochondrial oxidative phosphorylation. Surprisingly, FOXO1 did not stimulate but instead diminished oxidative metabolism as indicated by a decline in oxygen consumption in AdFOXO1^{CA}-expressing HUVECs (Fig. 3e). Moreover, reactive oxygen species (ROS) formation were decreased (Fig. 3f). Importantly, FOXO1 did not induce endothelial apoptosis, senescence, autophagy or energy distress under the same experimental conditions (Fig. 3g). Together, our data indicate that FOXO1 adapts metabolic activity to the lower requirements of the quiescent endothelium. To gain insight into the underlying mechanisms for this adaptability, we performed transcriptome analysis of FOXO1^{CA}- and GFP-transduced HUVECs. Gene set enrichment analysis (GSEA) revealed an enrichment of the FOXO1 DNA-binding elements in genes induced by FOXO1, while the MYC DNA-binding motif was highly enriched in the repressed genes (Fig. 3h). Moreover, MYC target gene signatures were downregulated in the FOXO1 transcriptome (Fig. 3i). Since MYC is a powerful driver of glycolysis, mitochondrial metabolism and growth[5], FOXO1 might antagonize endothelial MYC signalling. In line with this, overexpression of FOXO1^{CA} suppressed MYC expression and protein levels in HUVECs (Fig. 3j–l). Accordingly, numerous genes that are induced by MYC were downregulated in FOXO1^{CA}-overexpressing HUVECs, including genes involved in cell metabolism and cell cycle progression (Fig. 3i, l). This regulation is in line with the repression of MYC by FOXOs in cancer cells[5-7] and points to MYC as a crucial effector of FOXO1 in the coordination of endothelial metabolism and growth. Remarkably, FOXO1 also induced the expression of negative regulators of MYC signalling including MXI1, an antagonist of MYC transcriptional activity[8], and FBXW7, an E3 ubiquitin ligase that targets MYC for proteasomal degradation[8] (Fig. 3l). These data suggest that FOXO1 intersects with MYC signalling at different levels. To explore further the role of MYC in ECs, we analyzed the consequences of MYC inactivation for endothelial metabolism. Bioenergetic analysis revealed that MYC deficiency attenuated glycolysis and mitochondrial respiration (Fig. 4a, b). Conditional deletion of *Myc* (*Myc*$^{fl/fl}$)[9] in mice using the *Pdgfb-creERT2* deleter impaired vascular expansion and led to a thinned and poorly branched vasculature (Fig. 4c–e). These phenotypes resemble the vascular defects in *Foxo1*$^{iEC-CA}$ mutant mice and imply that MYC is a central component of endothelial FOXO1 signalling. To test this directly, we attempted to rescue the endothelial phenotypes imposed by FOXO1 activation by restoring MYC signalling with a Cre-inducible Myc overexpressor allele (*Myc*^{OE})[10]. *Pdgfb-creERT2*-induced overexpression of MYC caused sustained vascular overgrowth and led to a profound increase in EC number, proliferation and vessel density (Fig. 4f, g). We then combined the *Myc*^{OE}, *Foxo1*^{CA} and *Pdgfb-creERT2* alleles to generate endothelial-specific double mutants. Remarkably, re-expression of MYC in ECs of *Foxo1*$^{iEC-CA}$ mice normalized the hypobranched and hypocellular vascular phenotype caused by FOXO1 activation (Fig. 4h, i). Moreover, coexpression of MYC and FOXO1^{CA} in HUVECs restored glycolysis and mitochondrial respiration (Fig. 4j, k), indicating that regulation of MYC signalling by FOXO1 is critical for the coordination of endothelial metabolism and growth.

This study identifies FOXO1 as a critical checkpoint of endothelial growth that restricts vascular expansion. Our data suggest that FOXO1 promotes endothelial quiescence by antagonizing MYC, which leads to a coordinated reduction in the proliferative and metabolic activity of ECs. The FOXO1-induced deceleration of metabolic activity might not only enforce quiescence but also support endothelial function. For instance, by lowering metabolism, ECs will consume less energetic fuel for their homeostatic needs, thereby ensuring efficient nutrient and oxygen delivery. Reducing metabolic activity might also contribute to endothelial redox balance. ECs are long-lived cells that need to protect themselves against oxidative damage exerted by high oxygen levels in the bloodstream. The FOXO1-induced reduction in oxidative metabolism might thus be a mechanism to minimize the production of mitochondria-derived ROS, thereby conferring protection against the high-oxygen environment. Such a role of FOXO1 in endothelial metabolism aligns with the broader function of FOXOs in mediating oxidative stress resistance[11-13], and might also explain why ECs are exquisitely sensitive to a change in FOXO1 status. It will be interesting to determine how endothelial FOXO1 is regulated in vivo and how deregulation contributes to disease.

About the author

Kerstin Wilhelm (PhD)
Max Planck Institute for Heart and Lung Research, Angiogenesis & Metabolism Laboratory, Ludwigstraße 43, 61231 Bad Nauheim, Germany
E-mai: Kerstin.wilhelm@mpi-bn.mpg.de

10/2016 to Present: Postdoctoral fellow
Max-Planck Institute for Heart and Lung Research Bad Nauheim, Germany

11/2012 - 09/2016 PhD Student
Max Planck Institute for Heart and Lung Research Bad Nauheim, Germany
10/2010 - 10/2012 M.Sc. Molecular Medicine
Friedrich Schiller University, Jena, Germany

10/2007 - 09/2010 B.Sc. Biochemistry
University of Bayreuth, Bayreuth, Germany

Acknowledgement

Though only my name appears on the cover of this work, a great many people have contributed to its production. I owe my gratitude to all those people who have made this publication possible. Especially, I would like to express my sincere gratitude to my advisor Michael Potente for his support, motivation and enthusiasm. I'm deeply grateful for all his scientific inputs and discussions, as well as for the excellent environment that I experienced at the Max Planck Institute in Bad Nauheim.
I am also grateful to the Werner Risau Prize committee and the DGZ for recognizing my work. I feel honored being part of the vascular biology community, which Werner Risau pioneered.

Kerstin Wilhelm and Barbara Risau

References

1. De Bock, K., Georgiadou, M. & Carmeliet, P. Role of Endothelial Cell Metabolism in Vessel Sprouting. *Cell Metab.* **18**, 634–647 (2013).
2. Keller, C. et al. Alveolar rhabdomyosarcomas in conditional Pax3:Fkhr mice: cooperativity of Ink4a/ARF and Trp53 loss of function. *Genes Dev.* **18**, 2614–2626 (2004).
3. Sengupta, A., Chakraborty, S., Paik, J., Yutzey, K. E. & Evans-Anderson, H. J. FoxO1 is required in endothelial but not myocardial cell lineages during cardiovascular development. *Dev. Dyn.* **241**, 803–813 (2012).
4. Stöhr, O. et al. Insulin receptor signaling mediates APP processing and βamyloid accumulation without altering survival in a transgenic mouse model of Alzheimer's disease. *Age (Dordr)* **35**, 83–101 (2013).
5. Delpuech, O. et al. Induction of Mxi1-SR alpha by FOXO3a contributes to repression of Myc-dependent gene expression. *Mol. Cell. Biol.* **27**, 4917–4930 (2007).
6. Jensen, K. S. et al. FoxO3A promotes metabolic adaptation to hypoxia by antagonizing Myc function. *EMBO J.* **30**, 4554–4570 (2011).
7. Ferber, E. C. *et al.* FOXO3a regulates reactive oxygen metabolism by inhibiting mitochondrial gene expression. *Cell Death Differ.* **19**, 968–979 (2012).
8. Adhikary, S. & Eilers, M. Transcriptional regulation and transformation by Myc proteins. *Nat. Rev. Mol. Cell Biol.* **6**, 635–645 (2005).
9. de Alboran, I. M. et al. Analysis of C-MYC function in normal cells via conditional gene-targeted mutation. *Immunity* 14, 45–55 (2001).
10. Sander, S. *et al.* Synergy between PI3K signaling and MYC in Burkitt lymphomagenesis. *Cancer Cell* **22**, 167–179 (2012).
11. Kops, G. J. P. L. et al. Forkhead transcription factor FOXO3a protects quiescent cells from oxidative stress. *Nature* **419**, 316–321 (2002).
12. Tothova, Z. et al. FoxOs are critical mediators of hematopoietic stem cell resistance to physiologic oxidative stress. *Cell* **128**, 325–339 (2007).
13. Yeo, H. et al. FoxO3 coordinates metabolic pathways to maintain redox balance in neural stem cells. *EMBO J.* **32**, 2589–2602 (2013).

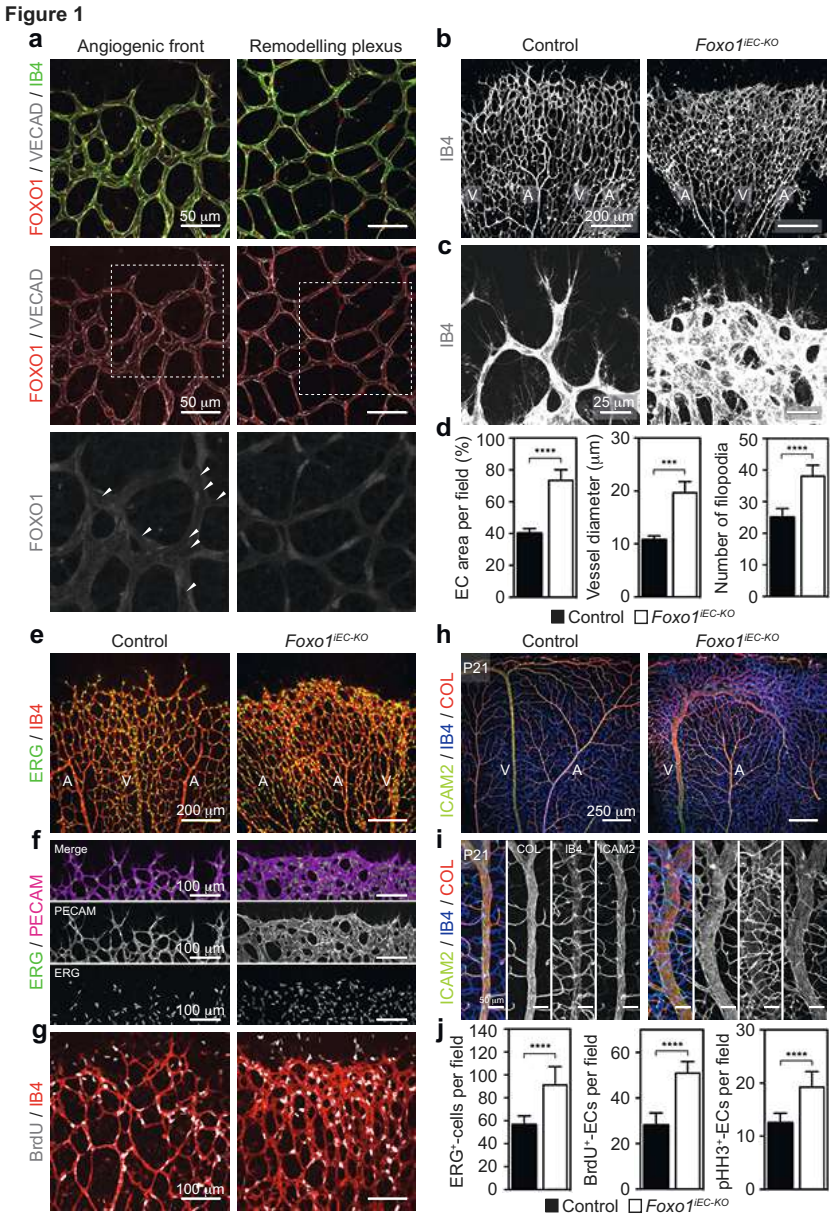

Figure 1 – Endothelial FOXO1 is an essential regulator of vascular growth.

a, Immunofluorescence staining for FOXO1 (red), VE-cadherin (VECAD; grey) and isolectin-B4 (IB4; green) in a P5 mouse retina. The lower panels depict the isolated FOXO1 signal (grey) of the boxed area shown in the middle panel. Note the diffuse nucleo-cytoplasmic localization of FOXO1 at the angiogenic front (left), while a stronger nuclear pattern is observed in the central remodelling plexus (right). Arrowheads point to ECs with weak FOXO1 nuclear staining. b,c, Overview (b) and higher magnification (c) confocal images of IB4-stained (grey) retinal vessels of P5 pups in *Foxo1*$^{iEC\text{-}KO}$ as compared to control (*Foxo1*$^{flox/flox}$) mice. A, artery; V, vein. d, Bar graphs showing the mean endothelial area (n ≥ 7), branch diameter (n ≥ 7), and number of filopodia per vessel length (n ≥ 5) in *Foxo1*$^{iEC\text{-}KO}$ mutant as compared to control (*Foxo1*$^{flox/flox}$) mice. Data represent mean ± s.d. Two-tailed unpaired *t*-test. e, Confocal images of IB4 (red) and nuclear ERG (green) stained P5 retinas of control and *Foxo1*$^{iEC\text{-}KO}$ mutant retinas showing the hyperplastic growth of *Foxo1*-deficient blood vessels. f, Confocal images of PECAM (magenta) and ERG (green) stained P5 retinas in control and *Foxo1*$^{iEC\text{-}KO}$ mice illustrating the clustering of ECs at the angiogenic front. g, BrdU (grey) and IB4 (red) labelling of whole-mount control and *Foxo1*$^{iEC\text{-}KO}$ P5 retinas. h,i, Overview (h) and higher magnification (i) confocal images of ICAM2 (green), IB4 (blue) and collagen IV (COL; red) stained retinas at P21 showing the venous enlargement in *Foxo1*$^{iEC\text{-}KO}$ mice. A, artery; V, vein. j, Quantifications of ERG/IB4- (n ≥ 9), BrdU/IB4- (n ≥ 5) and pHH3/IB4- (n ≥ 7) positive cells showing increased endothelial proliferation in the hyperplastic retinal vasculature of *Foxo1*$^{iEC\text{-}KO}$ mutant mice. Data represent mean ± s.d. Two-tailed unpaired *t*-test. Controls are Cre-negative littermates. ***$P < 0.001$; ****$P < 0.0001$.

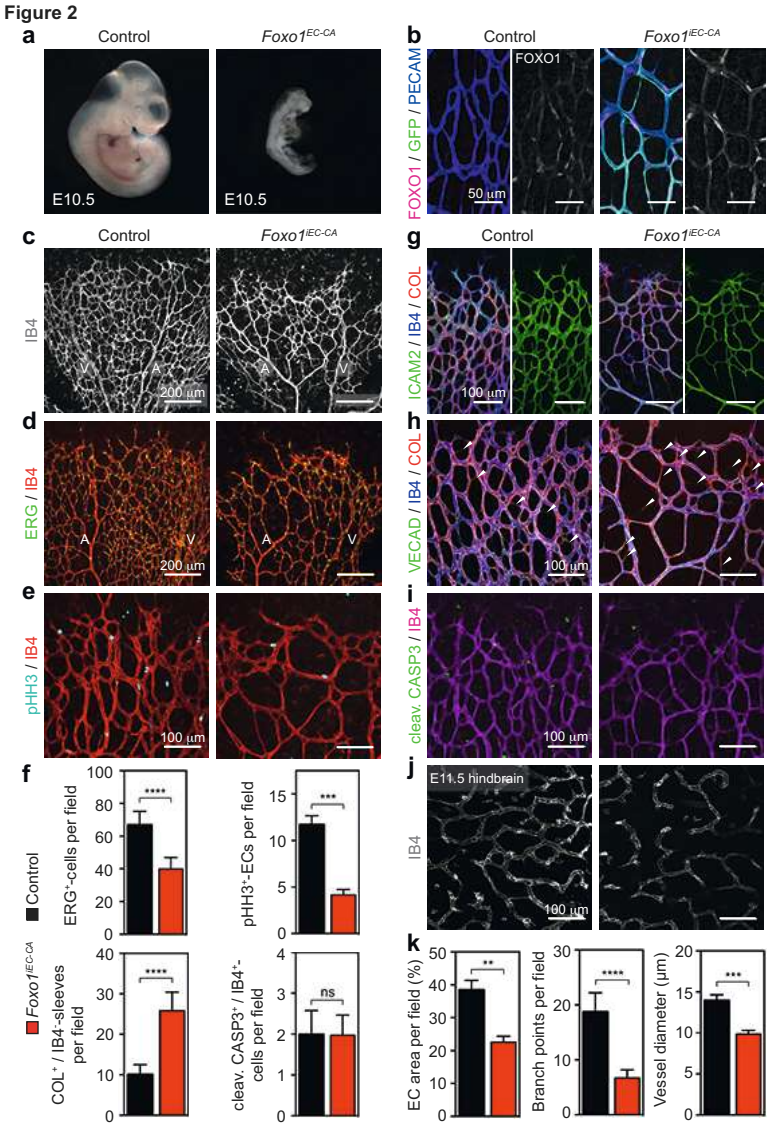

Figure 2 – Forced activation of FOXO1 restricts endothelial growth and vascular expansion

a, Overview images of freshly dissected E10.5 mouse embryos showing severe growth retardation in the constitutive *Foxo1*$^{EC\text{-}CA}$ mutants compared to control mice. b, Immunofluorescence staining for FOXO1 (magenta), GFP (green) and PECAM (blue) in P5 *Foxo1*$^{iEC\text{-}CA}$ and control mice. Note the enhanced nuclear FOXO1 signal in the GFP^{+}/PECAM^{+}-vessels. The right half of both images shows the FOXO1 staining (grey) alone. c, Confocal images showing the IB4-stained vasculature of P5 retinas in inducible *Foxo1*$^{iEC\text{-}CA}$ and control mice. A, artery; V, vein. d, Analysis of ERG- (green) and IB4- (red) stained P5 retinas in control and *Foxo1*$^{iEC\text{-}CA}$ mice illustrates a reduced number of ECs in the vasculature of *Foxo1*$^{iEC\text{-}CA}$ mice when compared to controls. e, IB4 (red) and pHH3 (cyan) labelling of whole-mount P5 retinas reveals reduced endothelial proliferation in *Foxo1*$^{iEC\text{-}CA}$ animals when compared to controls. f, Quantification of vascular parameters in the control and mutant retinas as indicated (n ≥ 5). Data represent mean ± s.d. Two-tailed unpaired *t*-test. g, Whole-mount ICAM2 (green), IB4 (blue) and COL (red) staining of retinas at P5 showing preserved luminal ICAM2 staining in *Foxo1*$^{iEC\text{-}CA}$ when compared to control. The right half of both images shows the ICAM2 staining (green) alone. h, Whole-mount triple immunofluorescence for VECAD (green), IB4 (blue) and COL (red) of P5 control and *Foxo1*$^{iEC\text{-}CA}$ retinas. The number of empty (COL^{+}, IB4^{-}-negative) sleeves (white arrows) in the retinal plexus is increased in the *Foxo1*$^{iEC\text{-}CA}$ mutants. i, Confocal images of IB4- (magenta) and cleaved Caspase 3 (CASP3; green) stained P5 retinas showing no difference in endothelial apoptosis between control and *Foxo1*$^{iEC\text{-}CA}$ mutant mice. j, IB4-stained (grey) E11.5 hindbrains following 4-OHT injection on E8.5 – E10.5 showing reduced vascularization in the ventricular zone of *Foxo1*$^{iEC\text{-}CA}$ mice. k, Quantification of EC area, vessel branch points and mean vessel diameter in control and *Foxo1*$^{iEC\text{-}CA}$ mutant hindbrains. Controls are littermate animals without cre (n ≥ 5). Data represent mean ± s.d. Two-tailed unpaired *t*-test. $^{**}P < 0.01$; $^{***}P < 0.001$; $^{****}P < 0.0001$.

Figure 3

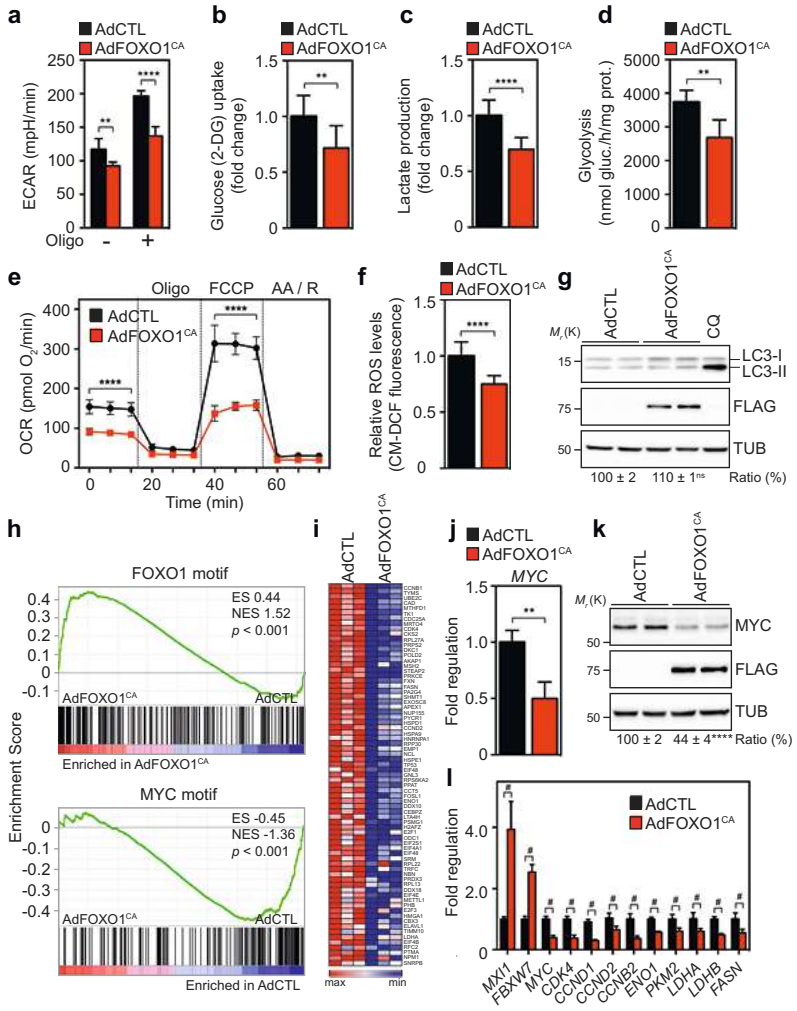

Figure 3 – FOXO1 slows endothelial metabolic activity and suppresses MYC signalling.

a, Extracellular acidification rate (ECAR), an indicator of glycolytic lactate production, in ECs treated with or without oligomycin (Oligo) showing reduced basal and maximal glycolytic activity in AdFOXO1^{CA}-transduced ECs when compared to control adenovirus- (AdCTL) transduced ECs (n = 6). Data represent mean ± s.d. Two-tailed unpaired t-test. b-d, Reduced uptake of the glucose analogue 2-deoxy-D-glucose (2-DG) (n = 13), decreased relative lactate production(n = 10) and lowered glycolytic flux (n = 4) in control and FOXO1^{CA}-expressing ECs. Data represent mean ± s.d. Two-tailed unpaired *t*-test. e, Oxygen consumption rates (OCR) in control and FOXO1^{CA}-overexpressing ECs under basal conditions and in response to oligomycin (Oligo), fluoro-carbonyl cyanide phenylhydrazone (FCCP) or antimycin A (AA) and rotenone (R). (n = 5). Data represent mean ± s.d. Two-way ANOVA with Bonferroni's multiple comparison test. f, Relative ROS levels in ECs 24 hours post transduction with AdCTL or AdFOXO1^{CA} (n = 7). Data represent mean ± s.d. Two-tailed unpaired *t*-test. g, Western blot analysis showing that overexpression of the Flag-tagged FOXO1^{CA} does not induce autophagy in ECs as the LC3-II to LC3-I ratio was not significantly changed. Chloroquine- (CQ) treated EC were used as a positive control. TUB, Tubulin. Densitometric quantifications 0 are shown below the lanes (n = 10). Data represent mean ± s.d. Two-tailed unpaired *t*-test. h, Gene set enrichment analysis of the FOXO1- (AAACAA) or MYC- (CACGTG) DNA binding element gene sets in AdFOXO1^{CA}- or AdCTL-transduced ECs. Note that the FOXO1 motif is enriched in the genes induced by AdFOXO-1^{CA}, while the MYC motif is enriched in the genes repressed by FOXO1. Black bars represent individual genes in rank order. ES, enrichment score, NES, normalized enrichment score. i, Heatmap of downregulated MYC signature genes in FOXO1^{CA}-overexpressing ECs (n=3). j,k, Analysis of MYC expression by microarray (j) and immunoblot (k) demonstrating the suppression of MYC in FOXO1^{CA}-Flag-overexpressing endothelium. The densitometric quantification of MYC protein levels is shown below the lanes of the immunoblot. (j, n = 6; k, n= 10). Data represent mean ± s.d. Two-tailed unpaired *t*-test. l, Quantitative polymerase chain reaction (qPCR) expression analysis of FOXO1^{CA}-regulated genes involved in MYC signalling. Relative mRNA levels are shown (n ≥ 3). Data represent mean ± s.d. Two-tailed unpaired *t*-test. *P < 0.05; **P < 0.01; ****P < 0.0001; #P < 00.1; ns, not significant.

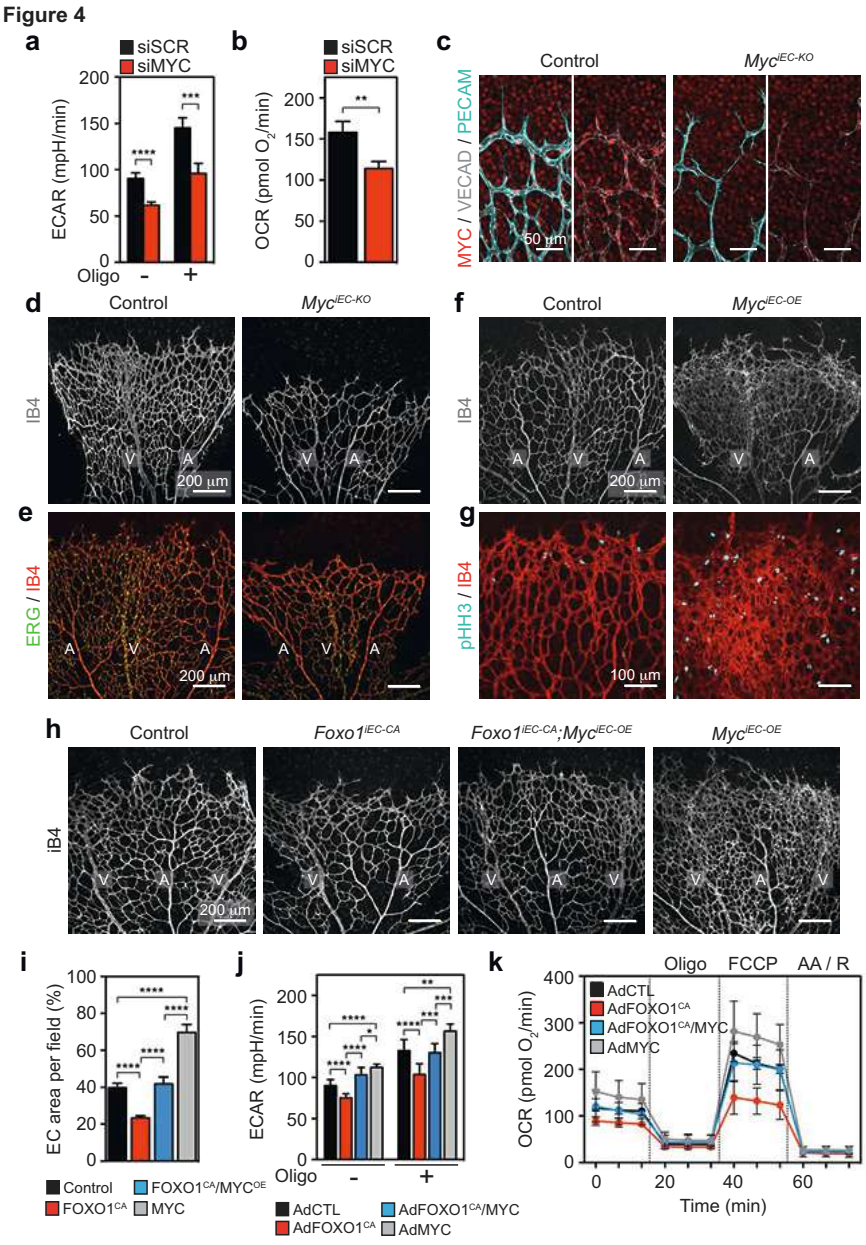

Figure 4 – MYC is a critical component of FOXO1 signalling in ECs.

a,b, ECAR (b) and OCR (c) in HUVECs showing a reduced metabolic activity in MYC siRNA- (siMYC) compared to SCR siRNA- (siSCR) transfected ECs (ECAR: n = 5; OCR: n = 5). Data represent mean ± s.d. Two-tailed unpaired *t*-test. c, Immunofluorescence staining for *MYC* (red), VECAD (grey) and PECAM (cyan) in P5 retinas of *Myc*$^{iEC-KO}$ and control mice. d, Confocal images of the IB4-stained vasculature in P5 retinas of *Myc*$^{iEC-KO}$ and control mice. A, artery; V, vein. e, Confocal images of IB4 (red) and nuclear ERG (green) stained P5 retinas of control and *Myc*$^{iEC-KO}$ mutant retinas showing a reduced number of ECs in the vasculature of *Myc*$^{iEC-KO}$ mice when compared to controls. f, Overview images of IB4-stained P5 retinal vessels in *Myc*$^{iEC-OE}$ and control mice. g, Enhanced EC proliferation in *Myc*$^{iEC-OE}$ mice as revealed by IB4 (red) and pHH3 (cyan) co-staining in P5 retinas. h,i, Confocal images of IB4-stained (grey) P5 retinas in control, *Foxo1*$^{iEC-CA}$, *Myc*$^{iEC-OE}$ and *Foxo1*$^{iEC-CA}$/*Myc*$^{iEC-OE}$ double mutants. Representative images (h) and quantification of endothelial coverage (i) in the respective genotypes are shown. Controls are littermate animals without cre expression (n ≥ 6 from 3 independent litters). Data represent mean ± s.d. One-way ANOVA with Bonferroni's multiple comparison post-hoc test. j,k, ECAR (j) and OCR (k) in AdCTL, AdFOXO1^{CA}, AdFOXO1^{CA}/AdMYC and AdMYC-transduced HUVECs showing the restoration of metabolic activity in FOXO1^{CA}/MYC co-expressing ECs (ECAR: n = 8; OCR: n ≥ 3). Data represent mean ± s.d. One-way ANOVA with Bonferroni's multiple comparison post-hoc test was performed in (j). $^{**}P < 0.01$; $^{***}P < 0.001$; $^{****}P < 0.0001$.